ChemComm

COMMUNICATION

View Article Online
View Journal | View Issue

Cite this: *Chem. Commun.*, 2024, **60**, 13024

Received 22nd August 2024,
Accepted 24th September 2024

DOI: 10.1039/d4cc04302b

rsc.li/chemcomm

Conformation matters: siRNAs with antisense strands with 5′-(*E*)-vinyl-phosphonate-α-L-LNA elicit stronger RNAi-mediated gene silencing than those with 5′-(*E*)-vinyl-phosphonate-LNA†

Dhrubajyoti Datta,[a] Pawan Kumar,[a] Soham Mandal,[b] Monika Krampert,[b] Martin Egli,[c] Patrick J. Hrdlicka[d] and Muthiah Manoharan*[a]

Conformationally constrained nucleotides, LNA or α-L-LNA, at the 5′ terminus of the antisense strand impeded gene silencing of small interfering RNA (siRNA) by hindering phosphorylation, thereby deterring loading into the RNA-induced silencing complex. Installation of a phosphate mimic, (*E*)-vinyl phosphonate (VP), improved activity considerably. Gene silencing was more efficient when the antisense strand of the siRNA was modified with 5′-VP-α-L-LNA, which adopts a C3′-*exo* (south) conformation, than when the antisense strand was modified with 5′-VP-LNA, which adopts a C3′-*endo* (north) pucker. These data underscore the critical role of conformation of nucleotides in RNA interference.

Therapeutics that act through the RNA interference (RNAi) pathway are a promising class of medicines, as demonstrated by the FDA approvals of several small interfering RNA (siRNA) drugs. Chemistry has played a crucial role in advancing these therapeutics as modified nucleotides are necessary to enhance metabolic stability, potency, and delivery to target tissues.[1,2]

The potency of an siRNA is influenced by the efficiency of loading of the antisense strand of the siRNA into the RNA-induced silencing complex (RISC); a 5′-phosphate is necessary for interaction with the MID domain of Ago2, the endonuclease component of RISC.[1–3] Oligonucleotides with 2′-OH or 2′-*O*-methyl (2′-OMe, Fig. 1, **I**) sugars are rapidly phosphorylated, but a synthetic phosphate mimic such as 5-(*E*)-vinyl phosphonate (5′-VP) must be incorporated in order for siRNAs with antisense strands ending with modifications such as 2′-*O*-methoxyethyl RNA, 2′–5′ DNA, 2′-*O*-[2-(methylamino)-2-oxoethyl] (2′-*O*-NMA) RNA, or 2′-deoxy-2′-α-F-2′-β-*C*-methyl (*gem*-2′-F/Me) RNA to be loaded into RISC (Fig. 1, **II–V**).[4–9] Recently, we evaluated siRNAs with antisense strands modified at the 5′ termini with the rigid bicyclic 2′-fluorinated northern-methanocarbacyclic (FNMC) sugar (Fig. 1, **VI**). siRNAs with the FNMC modification were not active even with the 5′-VP.[10] A key conclusion of our analysis of siRNAs modified with various sugar analogues was that a south-type conformation is critical for recognition by Ago2 and stable binding.[1,3,4,6–10]

The locked nucleic acid (LNA) modification has a methylene bridge that links the 2′ oxygen to the 4′ carbon of the RNA pentose ring, which fixes the pentose ring in the C3′-*endo* conformation (Fig. 2).[11,12] A diastereomer of LNA, α-L-LNA, locks the pentose ring in the C3′-*exo* conformation (Fig. 2).[13–18] The sugar conformations of LNA and α-L-LNA have been unequivocally established to be conformationally restricted in the C3′-*endo* and C3′-*exo* conformations, respectively, by NMR spectroscopy.[19,20] When incorporated into oligonucleotides, both LNA and α-L-LNA

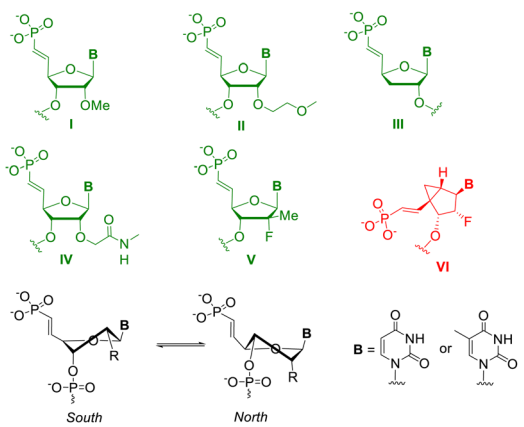

Fig. 1 The 5′-(*E*)-VP modified nucleotides previously tested in the context of siRNAs (**I–VI**) and conformational equilibrium between C2′-*endo* (south) and C3′-*endo* (north) sugars. R = 2′-modification.

[a] *Alnylam Pharmaceuticals, 675 West Kendall Street, Cambridge, MA 02142, USA. E-mail: mmanoharan@alnylam.com*
[b] *Axolabs GmbH, Fritz-Hornschuch-Strasse 9, 95326 Kulmbach, Germany*
[c] *Department of Biochemistry, School of Medicine Nashville, Vanderbilt University, TN 37232, USA*
[d] *Department of Chemistry, University of Idaho, Moscow, ID-83844, USA*

† Electronic supplementary information (ESI) available: New monomer building blocks and oligonucleotide characterization. See DOI: https://doi.org/10.1039/d4cc04302b

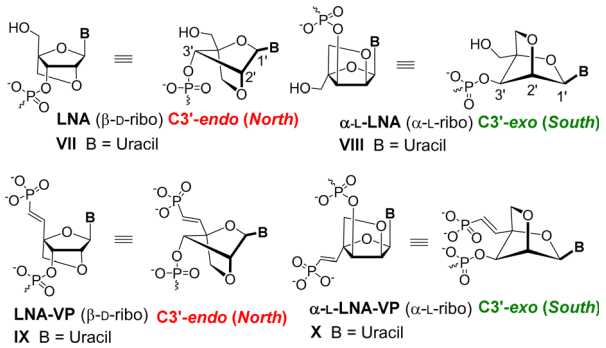

Fig. 2 Configurational and conformational features of LNA, α-L-LNA, and 5′-VP-functionalized LNA and α-L-LNA studied in this report.

modifications improve affinity for RNA and nuclease stability, and both modifications have been well-studied in the context of RNase H, splice modulation, miRNA antisense oligonucleotides, and aptamers.[11–18] In the present study, we investigated for the first time the impact of C3′-*endo* (north) LNA and C3′-*exo* (south) α-L-LNA incorporated at the 5′-terminus of the antisense strand, with and without 5′-VP, on the RNAi-based gene silencing activity of siRNA.

To synthesize the 5′-VP-LNA phosphoramidite, the 5′-OH group of commercially available nucleoside **1**[21] was oxidized by Dess–Martin periodinane to obtain **2**, which was then reacted with bis-pivaloyloxymethyl (POM) reagent to afford the POM-protected **3** through a Wittig-type reaction (Scheme 1). Deprotection of the *tert*-butyldimethylsilyl (TBS) group from **3** followed by the phosphitylation reaction afforded the 5′-VP-LNA-U phosphoramidite building block **5**. Similarly, 5′-VP-α-L-LNA-U phosphoramidite (**12**) was prepared from the corresponding α-L-LNA-U nucleoside (**6**) (Scheme 2). Reaction of **6**, prepared as described,[22] with TBS-chloride and imidazole in DMF, followed by treatment with aqueous trifluoroacetic acid in THF, afforded alcohol **8**. Oxidation of **8** using Dess–Martin periodinane provided aldehyde **9**, which was then converted to the POM-protected **10**. Removal of the 3′-*O*-TBDMS group from **10** followed by phosphitylation afforded phosphoramidite **12**. For both **5** and **12**, the *Z*-isomers were obtained as minor side products. As *Z*-isomers usually exhibit poor RNAi activity,[4,6–8] they were not included in this study.

POM-protected monomers **5** and **12**, as well as standard LNA **VII**,[23] α-L-LNA **VIII** (Scheme S1, ESI†), 2′-F-RNA, and 2′-OMe-

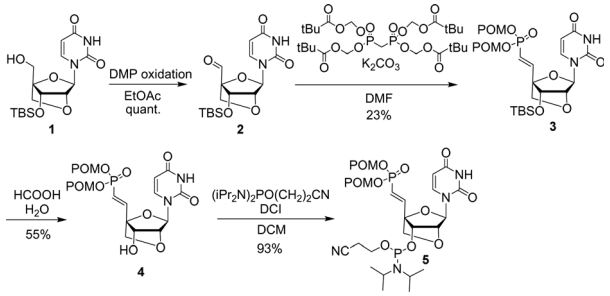

Scheme 1 Synthesis of 5′-VP-LNA-U phosphoramidite (**5**).

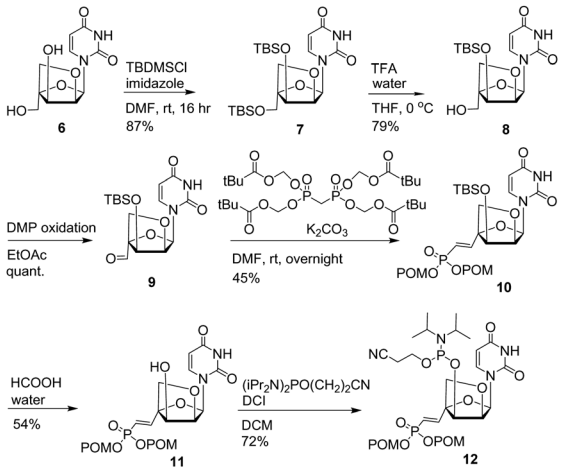

Scheme 2 Synthesis of 5′-VP-α-L-LNA-U phosphoramidite (**12**).

RNA phosphoramidites, were used to synthesize oligonucleotides *via* automated solid-phase oligonucleotide synthesis. When monomers **5** and **12** were incorporated, the final detritylation step was omitted. A one-step cleavage and deprotection was performed using aqueous ammonia containing 3% diethylamine (DEA). The crude oligonucleotides were purified by anion exchange HPLC and characterized by mass spectroscopy. The monomers were incorporated at the 5′ termini of antisense strands of siRNAs targeting mouse transthyretin (Ttr) (Table 1 and Table S1, ESI†). The sense strand was conjugated at the 3′ terminus to *N*-acetylgalactosamine (GalNAc). Strands were chemically modified as previously described.[1,2]

si-1 and **si-2** carry LNA (**VII**) and α-L-LNA U (**VIII**) monomers, respectively, at the 5′ end of the antisense strand; the 5′-most linkage is a natural phosphodiester. Controls included the siRNAs with antisense strands with a 5′-terminal 2′-OMe with phosphodiester or phosphorothioate linkages between the two

Table 1 siRNAs used in this study

No.	Sequences (5′-3′)	
	sense	antisense
si-1	a•a•*Ca*Gu*Gu**UCUu**Gc**Uc**Ua**Ua*AL	VII*U*•a*Ua*Ga*Gc*Aa*gaAcAc*Ug*Uu•u•u
si-2	a•a•*Ca*Gu*Gu**UCUu**Gc**Uc**Ua**Ua*AL	VIII*U*•a*Ua*Ga*Gc*Aa*gaAcAc*Ug*Uu•u•u
si-3	a•a•*Ca*Gu*Gu**UCUu**Gc**Uc**Ua**Ua*AL	u*U*•a*Ua*Ga*Gc*Aa*gaAcAc*Ug*Uu•u•u
si-4	a•a•*Ca*Gu*Gu**UCUu**Gc**Uc**Ua**Ua*AL	u•*U*•a*Ua*Ga*Gc*Aa*gaAcAc*Ug*Uu•u•u
si-5	a•a•*Ca*Gu*Gu**UCUu**Gc**Uc**Ua**Ua*AL	IX*U*•a*Ua*Ga*Gc*Aa*gaAcAc*Ug*Uu•u•u
si-6	a•a•*Ca*Gu*Gu**UCUu**Gc**Uc**Ua**Ua*AL	X*U*•a*Ua*Ga*Gc*Aa*gaAcAc*Ug*Uu•u•u
si-7	a•a•*Ca*Gu*Gu**UCUu**Gc**Uc**Ua**Ua*AL	VPu*U*•a*Ua*Ga*Gc*Aa*gaAcAc*Ug*Uu•u•u
si-8	a•a•*Ca*Gu*Gu**UCUu**Gc**Uc**Ua**Ua*AL	VPu•*U*•a*Ua*Ga*Gc*Aa*gaAcAc*Ug*Uu•u•u

Upper case italics indicate 2′-F RNA; lower case indicates 2′-OMe modification; VP indicates 5′-(*E*)-vinyl phosphonate; **VII–X** are modifications shown in Fig. 2; L indicates triantennary GalNAc; and • indicates phosphorothioate linkage.

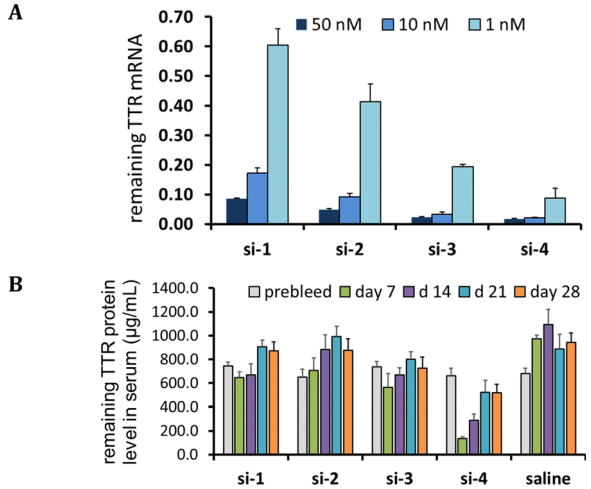

Fig. 3 siRNAs with LNA or α-L-LNA at the 5′ terminus of the antisense strands result in diminished silencing of gene expression in cultured cells or mice. (A) Ttr mRNA remaining in primary mouse hepatocytes cultured with the indicated siRNAs at the indicated concentrations under free uptake conditions. mRNAs were quantified by RT-qPCR, and averages ± standard deviations are plotted (n = 3). (B) Ttr protein amounts in serum at indicated days after mice were dosed subcutaneously with 1 mg kg^{-1} indicated siRNA. Plotted are averages ± standard deviations normalized to pre-dose levels in individual animals (n = 3).

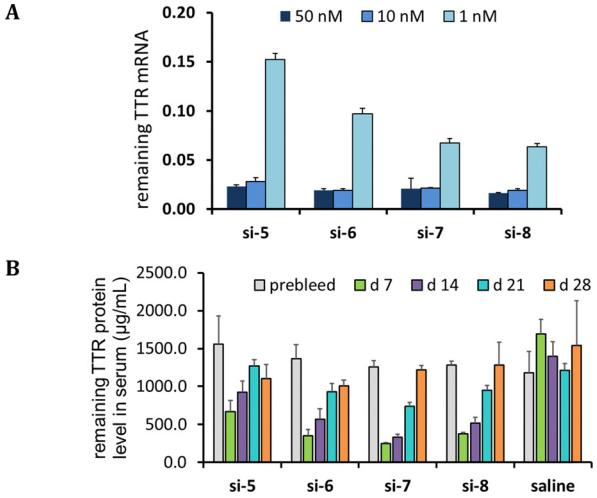

Fig. 4 The 5′-VP-α-L-LNA modification results in a more active siRNA than the 5′-VP-LNA modification. (A) Ttr mRNA remaining in primary mouse hepatocytes cultured with the indicated siRNAs at the indicated concentrations under free uptake conditions. mRNAs were quantified by RT-qPCR, and averages ± standard deviations are plotted (n = 3). (B) Ttr protein amounts in serum at indicated days after mice were dosed subcutaneously with 0.4 mg kg^{-1} indicated siRNA. Plotted are averages ± standard deviations normalized to pre-dose levels in individual animals (n = 3).

5′-terminal residues (**si-3** and **si-4**, respectively). In mouse primary hepatocytes under free uptake conditions, **si-1** and **si-2** were considerably less potent than the control **si-4** (Fig. 3A). The abilities of these siRNAs to reduce levels of serum Ttr in mice after a single subcutaneous dose of 1 mg kg^{-1} were also evaluated. Only **si-4** reduced levels of Ttr significantly (Fig. 3B). The phosphodiester linkage between N1 and N2 in **si-3** likely led to degradation and inactivity. We reason that kinase-catalyzed installation of phosphate groups on the bulky and conformationally restricted LNA and α-L-LNA 5′-terminal residues of **si-1** and **si-2** was impeded, resulting in diminished activity.

To test this hypothesis, we incorporated LNA and α-L-LNA monomers functionalized with the phosphate-mimicking 5′-VP at the 5′ termini of antisense strands of siRNAs. Under free-uptake conditions in primary mouse hepatocytes, the activities of siRNAs with antisense strands modified with 5′-VP-LNA and 5′-VP-α-L-LNA (**si-5** and **si-6**, respectively) were comparable to the controls in which the 5′ termini are 2′-OMe with a phosphodiester or phosphorothioate linkage (**si-7** and **si-8**, respectively) (Fig. 4A). In mice at a dose of 1.0 mg kg^{-1}, potencies of the siRNAs were similar, although **si-5** appeared to be slightly less potent (Fig. S1, ESI†). An additional experiment at a dose of 0.4 mg kg^{-1} confirmed that **si-6**, with the antisense strand modified with 5′-VP-α-L-LNA was more potent than **si-5**, modified with 5′-VP-LNA (Fig. 4B). Potencies of **si-6**, **si-7**, and **si-8** were comparable. That **si-7**, with a 5′-VP-2′-OMe with a phosphodiester linkage, was active is possibly due to the metabolic stability provided by the 5′-VP.

Next, we used computational modelling to evaluate how antisense strands modified with 5′-VP-LNA or 5′-VP-α-L-LNA interact with the Ago2 MID domain. A strand modified with 5′-VP-2′-OMe served as the reference structure (Fig. 5A)[3,24] (see ESI† for details). The 5′-VP-2′-OMe nucleotide adopts the C2′-*endo* sugar pucker as does the uridine in the parent structure.[3] The model of a strand with a 5′-phosphate α-L-LNA computed as a prelude to the 5′-VP model had a torsion angle β of −179.5°, ideal for replacing the phosphate with the 5′-VP, and the 5′-VP-α-L-LNA residue maintained all hydrogen-bonding interactions seen in the model with 5′-VP-2′-OMe (Fig. 5B). The α-L-LNA pucker is C3′-*exo* (south), a neighbour

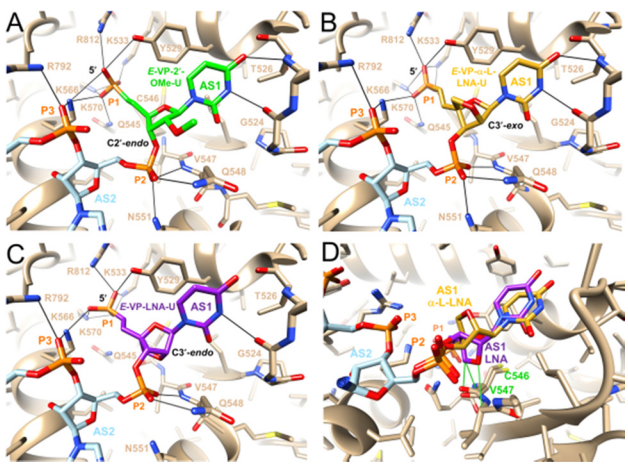

Fig. 5 5′-VP-α-L-LNA makes interactions with the Ago2 MID domain that are similar to those of the antisense strand modified with 5′-VP-2′-OMe. (A)–(C) Models of antisense strands modified with (A) 5′-VP-2′-OMe, (B) 5′-VP-α-L-LNA, and (C) 5′-VP-LNA lodged at the Ago2 MID domain binding site. (D) Overlay of 5′-VP-α-L-LNA (golden) and 5′-VP-LNA (violet) bound to the Ago2 MID domain.

range of C2′-*endo* in the pseudorotation phase cycle and therefore consistent with the preferred conformation for binding to the Ago2 MID domain.[1] This analysis is in complete agreement with the solution NMR analysis of α-L-LNA.[25]

The precursor model with 5′-phosphate LNA has a torsion angle β of +88° (sc+), not ideal for incorporation of 5′-VP (Fig. S2 in ESI†), and a north C3′-*endo* sugar pucker that required conformational adjustments within the nucleotide to accommodate the tight turn between the first two residues of the antisense strand necessary to establish optimal interactions with basic side chains of the MID and PIWI domains. Installing an 5′-VP moiety on the LNA residue and energy minimizing the model showed that it is possible to insert the phosphonate close to the locations of the corresponding moieties in the 5′-VP-2′-OMe model (Fig. 5C). However, the location of the phosphate in the 5′-LNA model is not as close to that in the crystal structure of Ago2 in complex with miR-20a as are the phosphonates in the 5′-VP-2′-OMe and 5′-VP-α-L-LNA models (Fig. S2 in ESI†). Crucially, the locked sugar of LNA has non-optimal contacts as short as 2.9 Å between its O2′–C5″ bridge and Ago2 main chain atoms of amino acids C546 and V547, which are located in a β-strand. As the overlay between the 5′-VP-α-L-LNA and 5′-VP-LNA models illustrates, a slight movement of the amide moiety away from the locked sugar bridge in the latter does not fully alleviate the short contacts that are below the sum of van der Waals radii of atoms involved (Fig. 5D).

In summary, we report syntheses of two new phosphoramidites, **5** and **12**, and their incorporation into oligonucleotides to introduce 5′-VP-LNA and 5′-VP-α-L-LNA modifications. When conformationally restricted LNA and α-L-LNA nucleotides were positioned at the 5′ end of the antisense strand, gene silencing activity was poor as was the case for the conformationally constrained FNMC modification.[10] The introduction of the 5′-VP modification in combination with α-L-LNA resulted in activity comparable to the siRNAs modified with a 5′-VP-2′-OMe. The siRNA modified with 5′-VP-LNA was less potent akin to VP-FNMC. Molecular modelling studies showed that the 5′-VP-α-L-LNA fits well within the Ago2 MID domain, maintaining all hydrogen-bonding interactions observed in the crystal structure with an unmodified RNA. Thus, the presence of conformationally constrained nucleotides at the 5′ terminus of the antisense strand impedes RNAi activity but installation of 5′-VP may result in RNAi activity if the 5′ nucleotide preorganizes the 5′-VP for favourable interaction with the MID domain. The α-L-LNA has a south pucker, the preferred conformation for Ago2 binding, whereas LNA, which has a rigid C3′-*endo* north pucker like FNMC, does not. Modification of the antisense strand with 5′-VP-α-L-LNA has the potential to expand the therapeutic utility of siRNAs. Furthermore, the 5′-VP modification was shown to provide sufficient metabolic stability to enable an antisense strand modified with 5′-VP-2′-OMe with a terminal phosphodiester linkage to attain comparable RNAi activity to an siRNA with a phosphorothioate linkage at that position.

This work is dedicated to Professors Takeshi Imanishi, Satoshi Obika, and Jesper Wengel for their contributions to development of Locked and Bridged Nucleic Acids (LNA and BNA).

Data availability

The data supporting this article have been included as part of the ESI.†

Conflicts of interest

There are no conflicts of interest to declare.

Notes and references

1 M. Egli and M. Manoharan, *Acc. Chem. Res.*, 2019, **52**, 1036–1047.
2 M. Egli and M. Manoharan, *Nucleic Acids Res.*, 2023, **51**, 2529–2573.
3 E. Elkayam, C. D. Kuhn, A. Tocilj, A. D. Haase, E. M. Greene, G. J. Hannon and L. Joshua-Tor, *Cell*, 2012, **150**, 100–110.
4 T. P. Prakash, W. F. Lima, H. M. Murray, W. Li, G. A. Kinberger, A. E. Chappell, H. Gaus, P. P. Seth, B. Bhat, S. T. Crooke and E. E. Swayze, *Nucleic Acids Res.*, 2015, **43**, 2993–3011.
5 W. Chang, Y. Pei, E. N. Guidry, D. Zewge, C. A. Parish, E. C. Sherer, J. DiMuzio, H. Zhang, V. J. South, W. R. Strapps, L. Sepp-Lorenzino, S. L. Colletti and M. G. Stanton, *Bioorg. Med. Chem. Lett.*, 2016, **26**, 4513–4517.
6 N. T. Schirle, G. A. Kinberger, H. F. Murray, W. F. Lima, T. P. Prakash and I. J. MacRae, *J. Am. Chem. Soc.*, 2016, **138**, 8694–8697.
7 E. Elkayam, R. Parmar, C. R. Brown, J. L. Willoughby, C. S. Theile, M. Manoharan and L. Joshua-Tor, *Nucleic Acids Res.*, 2017, **45**, 3528–3536.
8 R. G. Parmar, C. R. Brown, S. Matsuda, J. L. S. Willoughby, C. S. Theile, K. Charissé, D. J. Foster, I. Zlatev, V. Jadhav, M. A. Maier, M. Egli, M. Manoharan and K. G. Rajeev, *J. Med. Chem.*, 2018, **61**, 734–744.
9 D. C. Guenther, S. Mori, S. Matsuda, J. A. Gilbert, J. L. S. Willoughby, S. Hyde, A. Bisbe, Y. Jiang, S. Agarwal, M. Madaoui, M. M. Janas, K. Charisse, M. A. Maier, M. Egli and M. Manoharan, *J. Am. Chem. Soc.*, 2022, **144**, 14517–14534.
10 M. Akabane-Nakata, N. D. Erande, P. Kumar, R. Degaonkar, J. A. Gilbert, J. Qin, M. Mendez, L. B. Woods, Y. Jiang, M. M. Janas, D. K. O'Flaherty, I. Zlatev, M. K. Schlegel, S. Matsuda, M. Egli and M. Manoharan, *Nucleic Acids Res.*, 2021, **49**, 2435–2449.
11 S. Obika, D. Nanbu, Y. Hari, K.-I. Morio, Y. In, T. Ishida and T. Imanishi, *Tetrahedron Lett.*, 1997, **38**, 8735–8738.
12 S. Kauppinen, B. Vester and J. Wengel, *Drug Discovery Today Technol.*, 2005, **2**, 287–290.
13 V. K. Rajwanshi, A. E. Håkansson, B. M. Dahl and J. Wengel, *Chem. Commun.*, 1999, 1395–1396.
14 P. H. Hagedorn, R. Persson, E. D. Funder, N. Albæk, S. L. Diemer, D. J. Hansen, M. R. Møller, N. Papargyri, H. Christiansen, B. R. Hansen, H. F. Hansen, M. A. Jensen and T. Koch, *Drug Discovery Today*, 2018, **23**, 101–114.
15 V. K. Rajwanshi, A. E. Håkansson, M. D. Sørensen, S. Pitsch, S. K. Singh, R. Kumar, P. Nielsen and J. Wengel, *Angew Chem., Int. Ed.*, 2000, **39**, 1656–1659.
16 M. D. Sørensen, L. Kværnø, T. Bryld, A. E. Håkansson, B. Verbeure, G. Gaubert, P. Herdewijn and J. Wengel, *J. Am. Chem. Soc.*, 2002, **124**, 2164–2176.
17 P. P. Seth, A. Jazayeri, J. Yu, C. R. Allerson, B. Bhat and E. E. Swayze, *Mol. Ther. – Nucleic Acids*, 2012, **1**, e47.
18 P. Kumar, B. Baral, B. A. Anderson, D. C. Guenther, M. E. Østergaard, P. K. Sharma and P. J. Hrdlicka, *J. Org. Chem.*, 2014, **79**, 5062–5073.
19 K. E. Nielsen, S. K. Singh, J. Wengel and J. P. Jacobsen, *Bioconjug. Chem.*, 2000, **11**, 228–238.
20 K. M. E. Nielsen, M. Petersen, A. E. Håkansson, J. Wengel and J. P. Jacobsen, *Chem. – Eur. J.*, 2002, **8**, 3001–3009.
21 P. P. Seth and E. E. Swayze, WO2009124238, 2009.
22 P. Kumar, B. Baral, B. A. Anderson, D. C. Guenther, M. E. Østergaard, P. K. Sharma and P. J. Hrdlicka, *J. Org. Chem.*, 2014, **79**, 5062–5073.
23 A. A. Koshkin, S. K. Singh, P. Nielsen, V. K. Rajwanshi, R. Kumar, M. Meldgaard, C. E. Olsen and J. Wengel, *Tetrahedron*, 1998, **54**, 3607–3630.
24 E. Elkayam, C. R. Faehnle, M. Morales, J. Sun, H. Li and L. Joshua-Tor, *Mol. Cell*, 2017, **67**, 646–658.
25 J. T. Nielsen, P. C. Stein and M. Petersen, *Nucleic Acids Res.*, 2003, **31**, 5858–5867.